

224224: cordierite-bearing pelitic schist, Obelisk prospect (Yeneena Basin, Paterson Orogen)

Kelsey, DE, Duuring, P and Korhonen, FJ

Location and sampling

ANKETELL (SF 51-2), WEENOO (3256)

MGA Zone 51, 392767E 7718860N

Warox Site PZDOBL000001

Sampled on 18 November 2019

This sample was collected from the 248.5 – 248.7 m depth interval of diamond drillcore PND004, drilled by Sipa Resources Limited at their Obelisk Cu–Au prospect. The drillhole is located amongst dunes in the Great Sandy Desert part of the Paterson Orogen of Western Australia, about 350 km east of Port Hedland, 124 km north of Telfer minesite and 25 km south southwest of Citadel Hill.

Geological context

The unit sampled is a pelitic schist from the informally named Neoproterozoic ‘Anketell sediments’ of the Yeneena Basin in the Paterson Orogen (Czarnota et al., 2009). The northern parts of the Paterson Orogen, including at the Obelisk prospect, comprise metamorphosed Neoproterozoic rocks that are unconformably overlain by Phanerozoic sedimentary and volcanic rocks of the Canning Basin. Outcrop is poor, with most parts of the orogen covered by Quaternary sand dunes (Maidment, 2017). The sedimentary rocks within the Yeneena Basin were deposited after c. 923 Ma and are cut by 837–816 Ma mafic intrusions (Reed, 1996; Gardiner et al., 2018; Wingate et al., 2019a; Geoscience Australia sample GA2006677183, <www.ga.gov.au/geochron-sapub-web/geochronology/shrimp/search.htm>), and possibly 758–748 Ma mafic intrusions (Peter Haines, 2021, written comm., 10 June). The Rudall Province and Yeneena Basin are deformed by the 840–654 Ma Miles and 654–509 Ma Paterson Orogenies (Bagas, 2004; Kelsey et al., 2022b; Kelsey and Haines, 2022). Upright to inclined, east-southeast- to southeast-trending folds and southwest-directed thrusts are considered to be part of the Miles Orogeny and are locally cut by granitic rocks of the 654–603 Ma O’Callaghans Supersuite (Maidment, 2017). The Paterson Orogeny involved minor fault movement and folding during north-northeast–south-southwest shortening (Bagas, 2004). The Paterson Orogen hosts a diverse range of mineralization styles, including intrusion-related/orogenic Au–Cu (e.g. Telfer), sediment-hosted Cu (Nifty), vein and disseminated Cu–Au–Ag style (Winu), unconformity-associated U (Kintyre), skarn W–Cu–Zn (O’Callaghans) and possibly Mississippi Valley-type Pb–Zn (Warrabarty) deposits (Maidment et al., 2017). For the Obelisk prospect area regional airborne magnetic data and detailed gravity data suggest the presence of folded sedimentary rocks and mafic intrusions; emplacement of circular to weakly northwest-trending, magnetic and non-magnetic granitic rocks; and abundant north-northwest-trending dolerite dykes that cut the folded sedimentary and mafic igneous rocks, and granitic intrusions (Czarnota et al., 2009). Monazite from pelitic schist in the sample reported here yielded dates of 641 ± 3 Ma (GSWA 224224, Fielding et al., 2022). Monazite from pelitic schist in drillcore PND001 located 340 m to the west-northwest yielded dates of 645 ± 5 Ma (GSWA 239908, preliminary data). Molybdenite from a metagranitic vein that cuts pegmatitic vein within psammitic schist within drillcore PND001 yielded a Re–Os date of 651.6 ± 1.9 Ma (GSWA 224265, Wingate et al., 2021). Zircon from monzogranite and psammitic gneiss in drillcore T3 located 48 km to the north-northwest yielded dates of 649 ± 5 Ma for magmatic crystallisation (GSWA 214946, Wingate et al., 2019b) and 649 ± 5 Ma for metamorphism (GSWA 214945, Wingate et al., 2019c), respectively.

Petrographic description

The sample is a pelitic schist (Fig. 1) containing 45% muscovite, 26% quartz, 20% biotite, 4% plagioclase, 2% cordierite, 1% chlorite, 1% K-feldspar and accessory apatite, pyrrhotite, pyrite, monazite and zircon (Figs 1, 2; Table 1). The sample is characterized by biotite and muscovite that define a strong foliation, and quartz and lesser plagioclase, and features lens-shaped (augen) aggregates containing cordierite and unoriented biotite, muscovite, plagioclase, chlorite and quartz that are wrapped by the micaceous fabric (Figs 2, 3). Biotite in this sample is present in two distinct settings: within the strongly foliated matrix (M1) and as weakly foliated grains (M2) associated with quartz–feldspar±cordierite augen. Biotite grains are up to 500 μm long and appear unaltered. In backscattered electron (BSE) images, both M1 and M2 biotite exhibit homogeneous textures. Cordierite abundance in the lenses is low to very low. Minor K-feldspar occurs throughout the sample as anhedral grains typically <100 μm in size, as well as rare larger anhedral grains (~150 μm) located at or towards the margins of the augen containing cordierite. Chlorite occurs in low abundance in these cordierite-bearing domains and is interpreted as retrograde in origin because it partly mantles relict cordierite and is the expected low-temperature replacement of cordierite. Radiation damage halos from monazite and zircon are common in biotite.

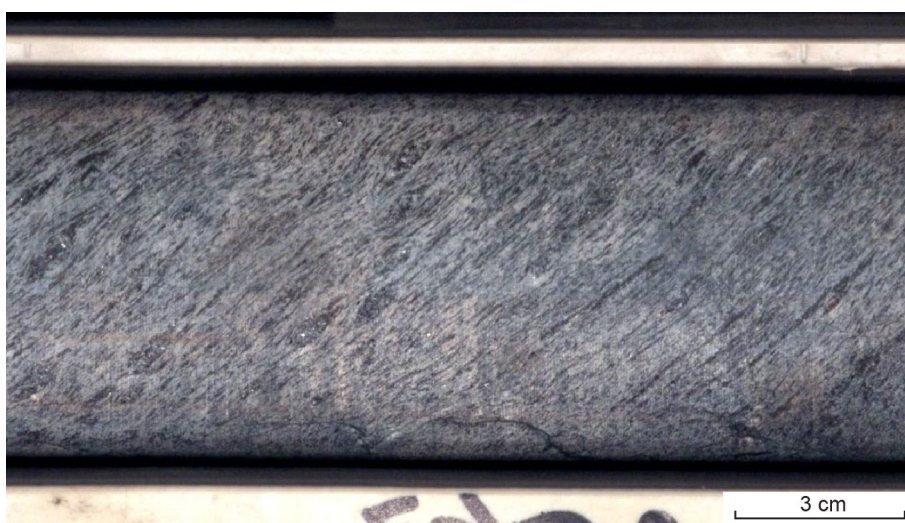


Figure 1. Drillcore image of sample 224224: cordierite-bearing pelitic schist, Obelisk prospect

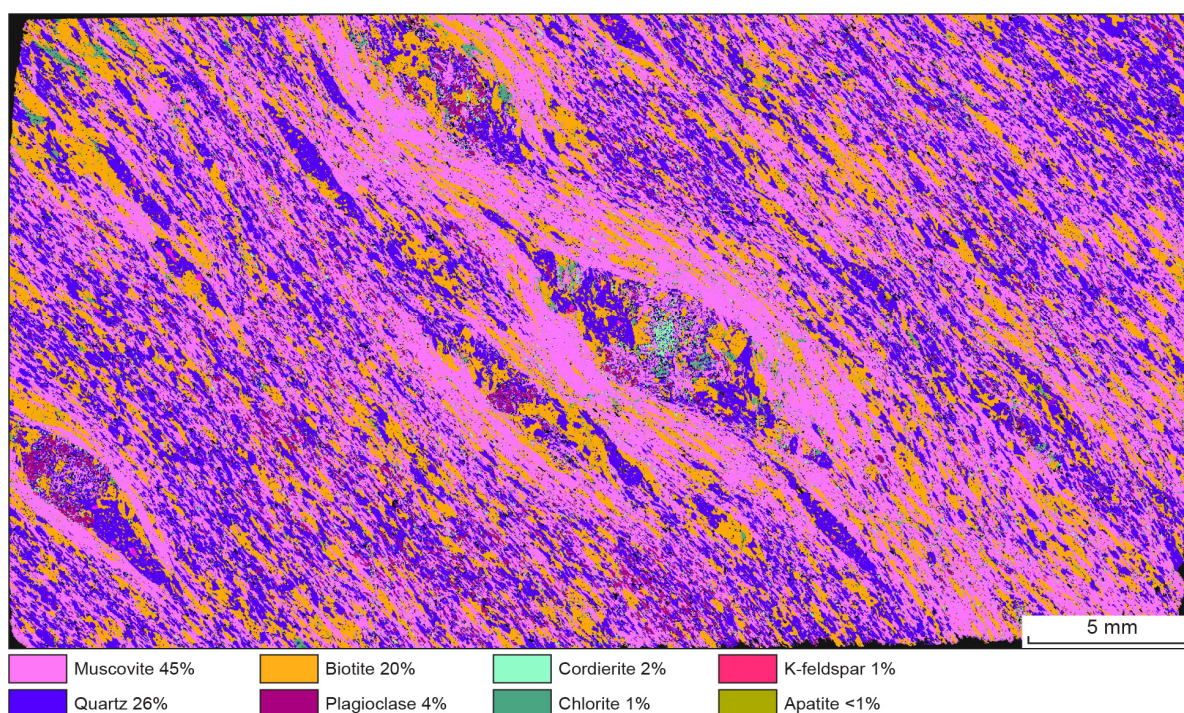
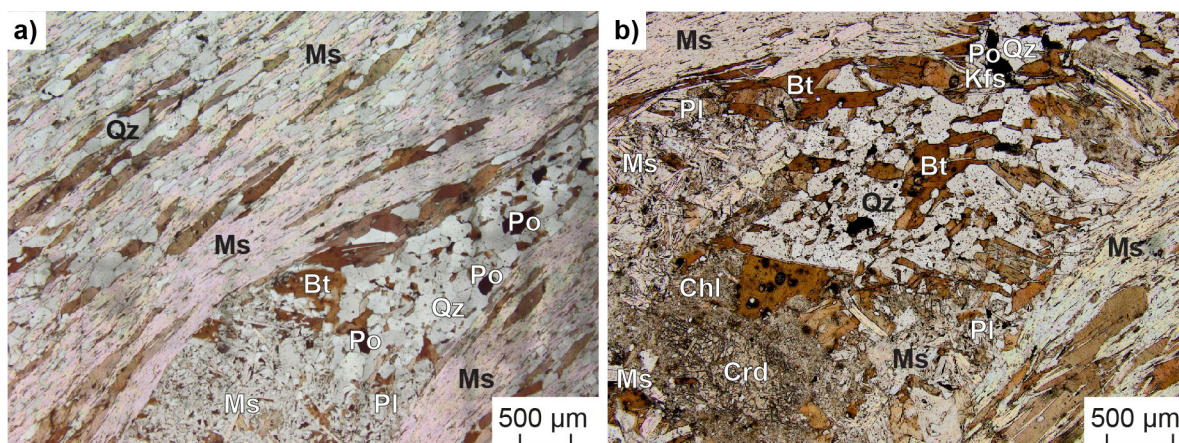


Figure 2. TESCAN Integrated Mineral Analyser (TIMA) image of an entire thin section from sample 224224: cordierite-bearing pelitic schist, Obelisk prospect. Volume percent proportion of major rock-forming minerals are calculated by the TIMA software

Table 1. Mineral modes for sample 224224: cordierite-bearing pelitic schist, Obelisk prospect

Mineral modes	Qz	Ms	Bt	Crd	Pl	Chl	Kfs	Rt	Ap	Po	Py
Observed (vol%)(a)	26	45	20	2	4	1	1	–	0.16	0.07	0.05
Predicted (mol%)											
@ 470 °C, 0.3 kbar	26	43	24	2	2	–	–	0.5	–	–	–
@ 580 °C, 1.6 kbar	26	43	25	3	4	–	–	0.3	–	–	–

NOTES: (a) trace monazite and zircon also present in thin section
– not present

**Figure 3. Photomicrographs in plane-polarized light, of sample 224224: cordierite-bearing pelitic schist, Obelisk prospect. Mineral abbreviations are explained in the caption to Figure 4, except for Po, pyrrhotite**

Analytical details

The metamorphic evolution of this sample was investigated using phase equilibria modelling, based on the bulk-rock composition (Table 2). The bulk-rock composition was determined by X-ray fluorescence spectroscopy, together with loss on ignition (LOI). The modelled O content (for Fe³⁺) was constrained as 2% of FeO on the basis of *T*–*M*₀ modelling (see Korhonen et al., 2020 for details) and the absence of Fe–Ti oxide minerals and presence of pyrrhotite. The sample is interpreted to be subsolidus and was modelled with H₂O in excess to create hydrated assemblages. The bulk composition was corrected for the presence of apatite and Fe-sulfide by applying a correction to calcium and iron, respectively (Table 2). Thermodynamic calculations were performed in the MnNCKFMASHTO (MnO–Na₂O–CaO–K₂O–FeO–MgO–Al₂O₃–SiO₂–H₂O–TiO₂–O) system using THERMOCALC version tc350 (updated June 2020; Powell and Holland, 1988) and the internally consistent thermodynamic dataset of Holland and Powell (2011; dataset tc-ds62, created in February 2012). The activity–composition relations used in the modelling are detailed in White et al. (2014a,b). Additional information on the workflow with relevant background and methodology are provided in Korhonen et al. (2020).

Table 2. Measured whole-rock and modelled compositions for sample 224224: cordierite-bearing pelitic schist, Obelisk prospect

XRF whole-rock composition (wt%)(a)												
SiO ₂	TiO ₂	Al ₂ O ₃	Fe ₂ O ₃	FeO ^(b)	MnO	MgO	CaO	Na ₂ O	K ₂ O	P ₂ O ₅	LOI	Total
56.88	0.91	22.01	--	5.79	0.07	3.11	0.41	0.59	7.00	0.13	2.64	99.54
Normalized composition used for phase equilibria modelling (mol%)												
SiO ₂	TiO ₂	Al ₂ O ₃	O ^(c)	FeO ^(d)	MnO	MgO	CaO ^(e)	Na ₂ O	K ₂ O	–	H ₂ O ^(f)	Total
57.09	0.69	13.02	0.05	4.72	0.06	4.65	0.26	0.58	4.48		14.43	100

NOTES: (a) Data and analytical details are available from the WACHEM database <<http://geochem.dmp.wa.gov.au/geochem/>>
(b) FeO analysed by Fe²⁺ titration; Fe₂O₃ content calculated by difference
(c) O content (for Fe₂O₃) adjusted
(d) FeO^T = moles FeO + 2 * moles O. Modified to remove pyrrhotite = moles FeO^T – (moles SO₂), where SO₂ moles = 0.151
(e) CaO modified to remove apatite: CaO(Mod) = CaO(Total) – (moles CaO(in Ap) = 3.33 * moles P₂O₅)
(f) H₂O content set as large amount so as to simulate ‘in excess’ scenario in modelling

Results

Metamorphic P – T estimates have been derived based on detailed examination of one thin section and the bulk-rock composition; care was taken to ensure that the thin section and the sample volume selected for whole-rock chemistry were similar in terms of featuring the same minerals in approximately the same abundances (Table 1), to minimize any potential compositional differences. The P – T pseudosection for sample 224224 was calculated over the range 0.2 – 3.0 kbar and 450–650 °C (Fig. 4). Cordierite is stable above about 450 °C; andalusite is stable above about 1.5 kbar and 510 °C and also (with K-feldspar) above about 500 °C at the lowest pressures, bound by a positively sloped reaction that results in the up-temperature disappearance of muscovite; chlorite occurs below ~450–540 °C at all pressures; the rutile–ilmenite reaction occurs at ~500–650 °C, to slightly higher temperature than the incoming of K-feldspar and andalusite, with ilmenite to higher temperature and rutile to lower temperature. Between about 500 and 600 °C the change from cordierite- to andalusite-bearing assemblages is strongly pressure sensitive. The presence of rutile, and possibly ilmenite, in the calculated phase equilibria, is attributed to the inability of the biotite activity–composition model to accommodate more Ti.

Interpretation

Based on the coarse grain size and mineral associations that support textural equilibrium, the peak metamorphic assemblage is interpreted to be muscovite–biotite–cordierite–plagioclase–quartz, which is stable (with rutile and H₂O in the pseudosection) up to 1.8 kbar and 450–590 °C. The predicted mineral modes (molar proportions approximately equivalent to vol%) across the peak field are broadly similar to the modes observed in the thin section (Table 1). The peak field is bound to lower temperature by the presence of chlorite and to higher temperature by the presence of K-feldspar, andalusite and ilmenite (Fig. 4). The absence of andalusite tightly constrains the maximum pressure for this sample to be ~1.8 kbar. In the pseudosection, the abundance of cordierite decreases to zero at slightly higher pressures (1.5–2 kbar) than the top of the peak assemblage field. The low abundance of cordierite in this sample suggests that pressures recorded by this sample were towards the top of the peak assemblage field where cordierite abundance is low. The presence of minor amounts of K-feldspar could indicate the P – T conditions occurred towards the high- T side of the peak field, proximal to or at the K-feldspar-in boundary. The presence of low amounts of chlorite in the sample is interpreted as recording the down-temperature, post-peak/retrograde, evolution of the rock. The peak P – T conditions are thermally extreme (e.g. Stüwe, 2007; Korhonen et al., 2020), defining apparent thermal gradients from ~330 to >2400 °C/kbar (within the near surface ultrahigh T/P thermal regime). Andalusite–cordierite-bearing pelitic schist sample GSWA 239908 (Kelsey et al., 2022a), located 340 m to the west-northwest (drillcore PND001), provides tighter P – T constraints of 1.3 – 1.8 kbar and 525–590 °C for peak metamorphism, which occur within the lower range of this apparent thermal gradient range. Such extreme apparent thermal gradient conditions are too high to be suggestive of regional metamorphism; instead they suggest local, shallow crustal contact metamorphism. As the pressures are so low for such high temperatures the P – T evolution path must be essentially isobaric.

Peak metamorphic conditions are estimated at 450–590 °C and a maximum pressure constraint of 1.8 kbar, with a minimum apparent thermal gradient of 330 °C/kbar. These conditions are consistent with local, shallow crustal contact metamorphism and a near isobaric P – T evolution path.

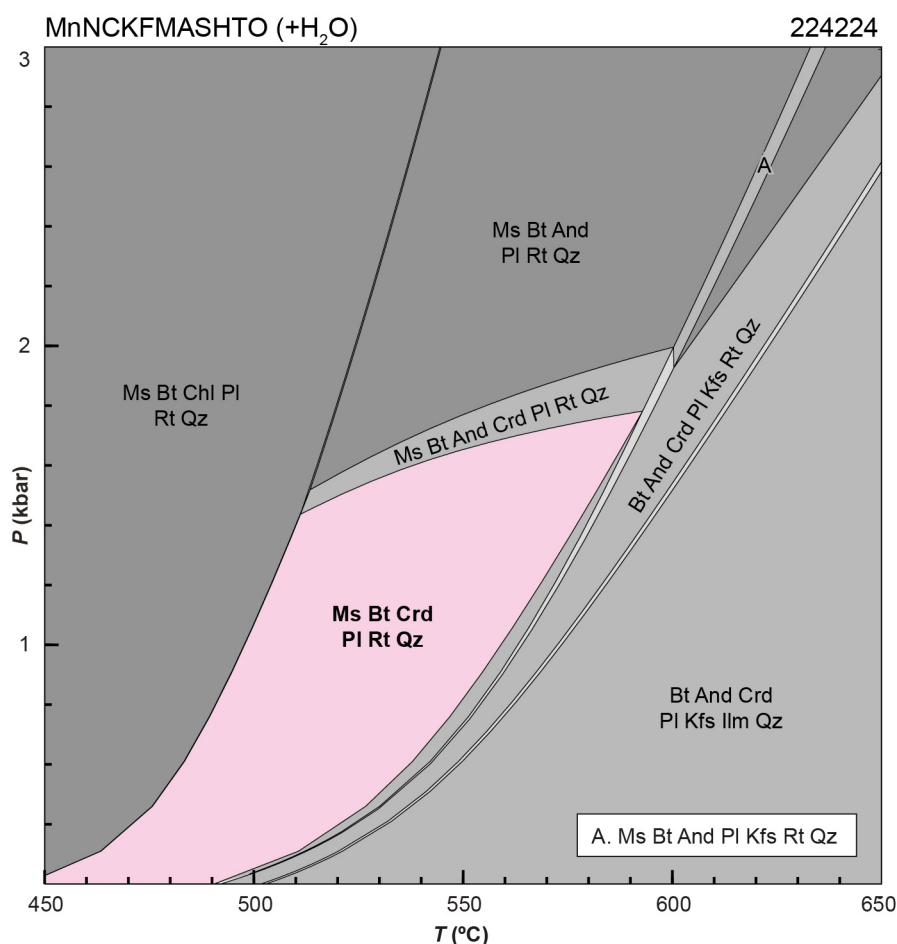


Figure 4. *P–T pseudosection calculated for sample 224224: cordierite-bearing pelitic schist, Obelisk prospect. Assemblage fields corresponding to peak metamorphic conditions are shown in bold text and pink shading. Abbreviations: And, andalusite; Bt, biotite; Chl, chlorite; Crd, cordierite; H₂O, fluid (pure H₂O); Ilm, ilmenite; Kfs, K-feldspar; Ms, muscovite; Pl, plagioclase; Qz, quartz; Rt, rutile*

References

- Bagas, L 2004, Proterozoic evolution and tectonic setting of the northwest Paterson Orogen, Western Australia: *Precambrian Research*, v. 128, p. 475–496.
- Czarnota, K, Berner, E, Maidment, DW, Meixner, A and Bagas, L 2009, Paterson Area 1:250 000 scale solid geology interpretation and depth to basement model, explanatory notes: Geoscience Australia, Record 2009/16, 89p.
- Fielding, IOH, Wingate, MTD, Duuring, P, Kelsey, DE, Rankenburg, K 2022, 224224: cordierite-bearing pelitic schist, Obelisk prospect; *Geochronology Record 1865: Geological Survey of Western Australia*, 5p.
- Gardiner, NJ, Maidment, DW, Kirkland, CL, Bodorkos, S, Smithies, RH and Jeon, H 2018, Isotopic insight into the Proterozoic crustal evolution of the Rudall Province, Western Australia: *Precambrian Research*, v. 313, p. 31–50.
- Holland, TJB and Powell, R 2011, An improved and extended internally consistent thermodynamic dataset for phases of petrological interest, involving a new equation of state for solids: *Journal of Metamorphic Geology*, v. 29, no. 3, p. 333–383.
- Kelsey, DE, Duuring, P and Korhonen, FJ 2022a, 239908: andalusite–cordierite-bearing pelitic schist, Obelisk prospect; *Metamorphic History Record 20: Geological Survey of Western Australia*, 7p.
- Kelsey, DE and Haines, PW 2022, Paterson Orogeny (PP): Geological Survey of Western Australia, WA Geology Online, Explanatory Notes extract, viewed 16 February 2022 <www.dmp.wa.gov.au/ens>.
- Kelsey, DE, Haines, PW and Duuring, P 2022b, Miles Orogeny (PM): Geological Survey of Western Australia, WA Geology Online, Explanatory Notes extract, viewed 16 February 2022 <www.dmp.wa.gov.au/ens>.
- Korhonen, FJ, Kelsey, DE, Fielding IOH and Romano, SS 2020, The utility of the metamorphic rock record: constraining the pressure–temperature–time conditions of metamorphism: *Geological Survey of Western Australia, Record 2020/14*, 24p.
- Maidment, DW 2017, *Geochronology from the Rudall Province, Western Australia: Implications for the amalgamation of the West and North Australian Cratons: Geological Survey of Western Australia, Report 161*, 95p.
- Maidment, DW, Huston, DL and Beardsmore, T 2017, Paterson Orogen geology and metallogeny, in *Australian Ore Deposits edited by GN Phillips: Australasian Institute of Mining and Metallurgy, Monograph 32*, p. 411–416.
- Powell, R and Holland, TJB 1988, An internally consistent dataset with uncertainties and correlations: 3. Applications to geobarometry, worked examples and a computer program: *Journal of Metamorphic Geology*, v. 6, no. 2, p. 173–204.

- Reed, A 1996, The structural, stratigraphic and temporal setting of the Maroochydore copper prospect, Paterson Orogen, Western Australia: The University of Western Australia, Perth, Australia, PhD thesis (unpublished), 289p.
- Stüwe, K 2007, Geodynamics of the lithosphere: An introduction: Springer, Berlin, 493p.
- White, RW, Powell, R, Holland, TJB, Johnson, TE and Green, ECR 2014a, New mineral activity-composition relations for thermodynamic calculations in metapelitic systems: *Journal of Metamorphic Geology*, v. 32, no. 3, p. 261–286.
- White, RW, Powell, R and Johnson, TE 2014b, The effect of Mn on mineral stability in metapelites revisited: New a–x relations for manganese-bearing minerals: *Journal of Metamorphic Geology*, v. 32, no. 8, p. 809–828.
- Wingate, MTD, Lu, Y and Haines, PW 2019a, 199495: metagabbro vein, Frankenstein 1: Geological Survey of Western Australia, Geochronology Record; Geochronology Record 1561: Geological Survey of Western Australia, 4p.
- Wingate, MTD, Lu, Y, Roche, LK and Haines, PW 2019b, 214946: monzogranite, Citadel Project; Geochronology Record 1565: Geological Survey of Western Australia, 6p.
- Wingate, MTD, Lu, Y, Roche, LK and Haines, PW 2019c, 214945: psammitic gneiss, Citadel Project; Geochronology Record 1564: Geological Survey of Western Australia, 8p.
- Wingate, MTD, Creaser, RA, Duuring, P and Lu, Y 2021, 224265: molybdenite-bearing vein, Obelisk prospect; Geochronology Record 1728: Geological Survey of Western Australia, 3p.

Links

Metamorphic history introduction document: [Intro_2020.pdf](#)

Recommended reference for this publication

Kelsey, DE, Duuring, P and Korhonen, FJ 2022, 224224: cordierite-bearing pelitic schist, Obelisk prospect; *Metamorphic History Record* 17: Geological Survey of Western Australia, 6p.

Data obtained: 15 October 2020

Date released: 14 April 2022

This Metamorphic History Record was last modified on 29 March 2022.

Grid references in this publication refer to the Geocentric Datum of Australia 1994 (GDA94). All locations are quoted to at least the nearest 100 m.

WAROX is GSWA's field observation and sample database. WAROX site IDs have the format 'ABCXXXnnnnnnSS', where ABC = geologist username, XXX = project or map code, nnnnnn = 6 digit site number, and SS = optional alphabetic suffix (maximum 2 characters).

Isotope and element analyses are routinely conducted using the GeoHistory laser ablation ICP-MS and Sensitive High-Resolution Ion Microprobe (SHRIMP) ion microprobe facilities at the John de Laeter Centre (JdLC), Curtin University, with the financial support of the Australian Research Council and AuScope National Collaborative Research Infrastructure Strategy (NCRIS). The Tescan Integrated Mineral Analyser (TIMA) instrument was funded by a grant from the Australian Research Council (LE140100150) and is operated by the JdLC with the support of the Geological Survey of Western Australia, The University of Western Australia (UWA) and Murdoch University. Mineral analyses are routinely obtained using the electron probe microanalyser (EPMA) facilities at the Centre for Microscopy, Characterisation and Analysis at UWA, and at Adelaide Microscopy, University of Adelaide.

Digital data related to WA Geology Online, including geochronology and digital geology, are available online at the Department's Data and Software Centre and may be viewed in map context at [GeoVIEW.WA](#).

Disclaimer

This product uses information from various sources. The Department of Mines, Industry Regulation and Safety (DMIRS) and the State cannot guarantee the accuracy, currency or completeness of the information. Neither the department nor the State of Western Australia nor any employee or agent of the department shall be responsible or liable for any loss, damage or injury arising from the use of or reliance on any information, data or advice (including incomplete, out of date, incorrect, inaccurate or misleading information, data or advice) expressed or implied in, or coming from, this publication or incorporated into it by reference, by any person whatsoever.



© State of Western Australia (Department of Mines, Industry Regulation and Safety) 2022

With the exception of the Western Australian Coat of Arms and other logos, and where otherwise noted, these data are provided under a Creative Commons Attribution 4.0 International Licence. (<http://creativecommons.org/licenses/by/4.0/legalcode>)

Further details of geoscience products are available from:

Information Centre
Department of Mines, Industry Regulation and Safety
100 Plain Street
EAST PERTH WA 6004
Telephone: +61 8 9222 3459 | Email: publications@dmirs.wa.gov.au
www.dmirs.wa.gov.au/GSWApublications